Effectiveness Factors in a Nonisothermal Reaction System

R. A. CUNNINGHAM, J. J. CARBERRY, and J. M. SMITH

University of California, Davis, California

Hydrogenation rates of ethylene on a copper-magnesium oxide catalyst were measured for fine catalyst particles and ½ in. spherical pellets from 60° to 160°C. Experimental effectiveness factors for this exothermic reaction system ranged from 0.2 to 25, depending upon the temperature and density of the catalyst pellets. The activation energy for the particles was 11,800 cal./g. mole (above 120°C.), while E for the pellets decreased to zero at high temperatures. Reasons for this behavior are discussed.

The effective thermal conductivity of the catalyst pellets was measured as a function of density and the effective diffusivity was estimated from pore size and pore volume measurements. In principle this information and the rate data for the particles are sufficient to predict effectiveness factors for the pellets. However available prediction methods are based upon first or second order rate equations which do not fit the ethylene hydrogenation reaction.

When a gaseous reaction occurs on a porous catalyst, concentration, temperature, and pressure gradients may exist within individual catalyst pellets. As a result the average rate of reaction over the entire catalyst area is not, in general, equal to the rate at the conditions of the external surface of the pellet. The ratio of these two rates has been termed the effectiveness factor η. Under isothermal, constant pressure conditions the only effect is the reduction in concentration within the pellet and this gives rise to η values less than unity. Theoretical methods of treating this case for various types of reactions have been considered by Thiele (*29*), Damkoeler (*7, 8*), Zeldovich (*40*), Wagner (*32*), Wheeler (*38*), Weisz (*35*), Kubota and Shindo (*15*), and Carberry (*3*), among others. When the heat of reaction is significant, the temperature increases (for an exothermic reaction) with penetration, owing to the finite thermal conductivity of the catalyst pellet. This normally causes η to increase. Damkoeler (*7*) and Prater (*22*) have shown that this temperature change can be sufficient to produce a large increase in rate of reaction. The combined effects of concentration and temperature gradients upon the effectiveness factors have been studied analytically and numerically by several investigators (*14, 24, 30, 31, 4, 19, 37*). In principle the effectiveness factor for an autothermic reaction can increase without limit and also can have more than one value at fixed conditions because of the existence of two stable states (*37, 11, 2*). However, extraparticle diffusion resistance will begin to modify intraparticle predictions as the effectiveness factor increases (*4*).

The purpose of this study was to measure intrapellet temperature gradients and also to obtain sufficient data to evaluate experimental effectiveness factors. To do this rate data were observed for the hydrogenation of ethylene on a copper-magnesium oxide catalyst in the form of granular particles (100 to 150 Tyler mesh) and ½ in. spherical pellets. The reaction is moderately exothermic ($\Delta H_{298°}$ = − 32,700 cal./g. mole). The feed mixture to the reactors contained less than 17 mole % ethylene (remainder hydrogen) so that the change in total moles within the catalyst pellets was small. This reduced the variation in total pressure and its effect on the rate of reaction. These items are of interest because a second objective was to compare experimental E values with those calculated from the prediction methods for nonisothermal systems. Such methods suppose first-order surface kinetics and no pressure gradient within a pellet.

To predict numerical results requires, in addition to surface rate data, a knowledge of the effective diffusivity and thermal conductivity. The former quantity can be estimated (*33*) from pore volume and pore size measurements, and these were measured for the catalyst pellets. The procedure of calculating diffusivities presupposes the absence of surface diffusion. This is commonly assumed but to the authors' knowledge has not been demonstrated at conditions of catalytic reactions. Accurate means of estimating the effective thermal conductivity have not been developed. Hence approximate values of k_e were measured.

EXPERIMENTAL

Reaction Apparatus

The hydrogenation apparatus is shown schematically in Figure 1. Electrolytic grade hydrogen (99.8% purity, 0.15% oxygen, 0.049% nitrogen) flowed through a 3 ft. long section of ¼ in. galvanized pipe packed with the copper-magnesium oxide catalyst. This converter was operated at 250°C. to re-

R. A. Cunningham is on leave from University of Buenos Aires as a Fellow of the Consejo National de Argentina. J. J. Carberry is at Notre Dame University, Notre Dame, Indiana.

move the small amount of oxygen. After cooling the gas was dehydrated in a ¼-in. iron pipe packed for length of 3 ft. with silica gel. The ethylene (99.7% purity, ethane 0.1%, propane 0.1%, and propylene 0.1%) was first passed through a converter filled with copper shot and operated at 250°C. to eliminate any oxygen that might be present. Following this the ethylene was cooled and dehydrated.

The flow rates of the two gases were determined separately in capillary flow meters and then combined in a glass jet mixer. From the mixer the reactants passed directly to one of the two reactors. For measuring the rate of reaction of catalyst particles a 7-mm. I.D. glass U tube was employed as illustrated in Figure 2. Two iron-constantan, 24-gauge thermocouples were inserted along the central axis of the catalyst bed, and three similar thermocouples were attached with epoxy resin to the outside of the reactor wall adjacent to the catalyst bed. The inner couples were placed at positions corresponding to 0.07 and 0.72 of the total bed length; the distance between the couples was 2.7 cm. The extreme outer couples were adjacent to the entrance and exit of the catalyst bed and the third at a position corresponding to 0.31 of the bed length. Entrance and exit sections packed with 2-mm. glass beads were employed. The catalyst particles were supported on a 1-cm. section of very small glass particles (average diameter = 0.08 mm.).

For studying pellets a glass tank-flow reactor (Figure 2) was used. The feed entered at the bottom through a glass nozzle to produce turbulence around the catalyst pellet. Three thermocouples, iron-constantan, 24-gauge, were employed to record the center and surface temperatures of the pellet and the temperature in the surrounding gas. The inlet tube contained a section of glass beads to aid in preheating the feed to the reaction temperature.

The reactors were immersed in a constant temperature bath in which the temperature could be controlled to 0.5°F. Conversion in the tubular reactor was limited to a few percent in order to reduce temperature and composition variations along the bed. The average difference in temperature in the radial direction in the catalyst bed was about 3°C., while that in the axial direction was about 8°C. The method of correcting for these variations is described later.

A thermal conductivity cell (4 filament, 30-S geometry), operated at a constant current of 140 mamp., was used to determine the conversion. The reactants stream served as the reference gas (Figure 1) so that the unbalanced voltage from the cell was a measure of the conversion. The cell was maintained at approximately 25°C. in an insulated box and calibrated by preparing synthetic mixtures of ethane, ethylene, and hydrogen.

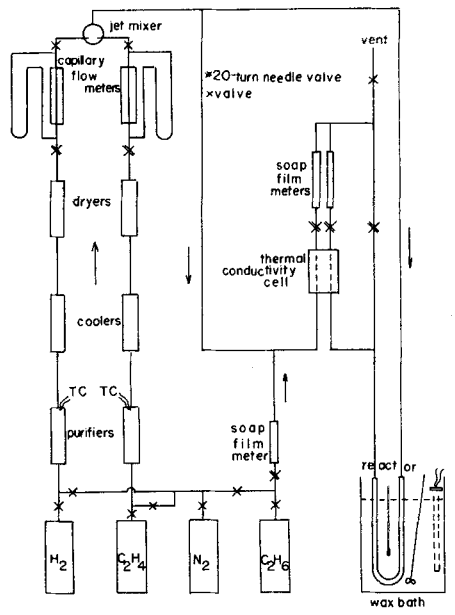

Fig. 1. Schematic diagram of apparatus.

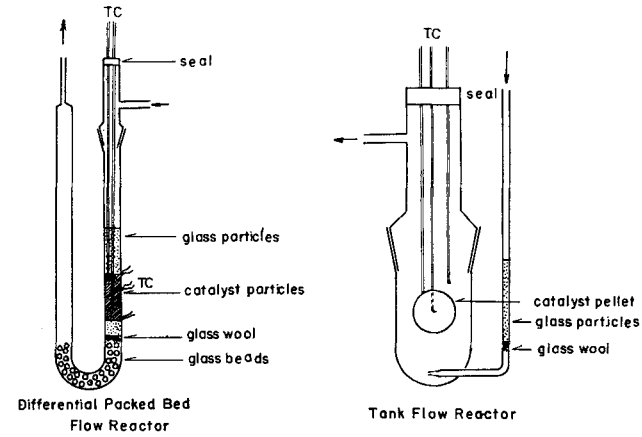

Fig. 2. Reactor details.

Catalyst Preparation

The reverse technique of Taylor (*26, 27*) was employed to make the catalyst. Similarly prepared materials have been used by others (*28, 39*) for the hydrogenation of ethylene. A single, equal-molal batch was prepared by dissolving electrolytic copper in nitric acid and adding magnesium nitrate. The nitrates were precipitated with 1N sodium hydroxide. The precipitate was filtered, dried at 110°C. for 48 hr., and then calcined for 10 days at 240°C. After grinding to 100 mesh size these particles were used as the unreduced catalyst for all the rate studies.

Spherical pellets, ½-in. diameter, were prepared by compressing the unreduced particles in a steel mould. To permit removal of the pellet from the mould, the metal surfaces were lubricated with stearic acid which evaporated later during the reduction process. A small hole was drilled radially to the center of the pellet for insertion of the thermocouple. The slight space between the wires and the hole wall was filled with catalyst particles, and the mouth was sealed with a drop of epoxy resin. For measurement of surface temperature, the thermocouple was inserted into a small cavity formed on the spherical surface. The couple was pressed lightly into the catalyst and sealed in place with a small drop of epoxy resin.

PHYSICAL PROPERTIES OF CATALYST

The macropores (pores for which $a > 150$Å) characteristics of the pellets were measured for both unreduced (see Section on Catalyst Pretreatment) and used catalysts with a mercury porosimeter. These results are summarized in Table 1. The macrovoid fraction was determined from the volume of mercury penetrating the sample and its total volume. Mean pore radii were established for pellets of each density from the equation

$$\overline{a_a} = \frac{\int_o^{V_a} a_a dV_a}{V_a} \qquad (1)$$

These values are necessary to estimate the Knudsen diffusion contribution in the pores, and Equation (1)has been derived (*33*) to give a correct average radius for Knudsen diffusion in the macropores.

Pellets of three different densities (ρ_B) were prepared by compressing different masses of catalyst particles in the mould. The macropore void fraction and volume decrease as the density increases, as shown in Table 1. The data in the table that depend upon mass are based upon the weight of unreduced catalyst. For pellets of the same density the void fraction is less for the used catalyst. This is due to the deposit of carbonaceous material during initial use. It is noted that this difference is greatest for the lowest density and approaches zero for the pellet of greatest density. The particle density ρ_p is equal to pellet density divided by $1 - \epsilon_a$. If ρ_p for pellets of different

TABLE 1. PHYSICAL PROPERTIES OF CATALYSTS

Pellet density,*	Macropores			Micropores			Particle density,*	Surface area, S_g,*	Carbon deposition, g./g.	
ρ_B, g./cc.	V_{ga},* cc./g.	ϵ_a	$\bar{a}_a$, Å	V_{gi},* cc./g.	ϵ_i	$\bar{a}_i$, Å	ρ_p, g./cc.	sq. m./g.	Max.	Min.
					Used catalyst					
1.19	0.26	0.34	300						0.22	0.08
1.16	0.21	0.25	300	0.236	0.28	88.5	2.14	90	0.13	0
0.95	0.32	0.34	600						0.33	0.20
0.72	0.30	0.32	1170	0.046	0.033	41.2		8.3	0.60	0.47
					Unreduced catalyst					
1.16	0.26	0.25	300	0.236	0.28	88.5	2.14	90		
0.95	0.54	0.55	600		0.22		2.26			
0.72	0.92	0.67	1200		0.17		2.18			

* Based upon mass of unreduced catalyst.

densities is the same, the pelleting process did not crush the particles. This comparison is shown in Table 1 for the unreduced catalyst. A similar comparison is not possible for the used pellets because deposition of carbonaceous material changes the calculated particle density.

The micropore (pores for which $a < 150$Å) void volume was evaluated in a sorptometer. Samples studied were used pellets of greatest density (little or no carbon deposition) and lowest density (greatest carbon deposition), and unreduced pellet of lowest density. The micropore void fraction is equal to $\rho_B V_{gi}$. The average micropore radius $\bar{a}_i$ was evaluated by an expression identical with Equation (1), except the integration is carried out over the micropore region. The surface area, as evaluated from the B.E.T. equation and the sorptometer data, decreased sharply with carbon deposition, as shown in Table 1.

The carbon deposition (grams of carbon per gram of unreduced catalyst) is also given in Table 1 for each used catalyst pellet. This was calculated by weighing the pellet after removal from the reactor. The weight of the unused but reduced catalyst is also known from the weight of the original unreduced sample, and the amount of oxygen that is eliminated by reduction. This is determined by assuming that the copper oxide is completely reduced. Now the amount of carbon can be calculated by subtracting the weight of the reduced, unused catalyst from the weight of the used pellet. A minimum carbon deposition is obtained if the reacted pellet is assumed to reoxidize completely in air upon removal from the reactor. A maximum carbon deposition is calculated if the used catalyst is supposed to remain unoxidized. The actual result is judged to be closer to the minimum value, although both are given in Table 1.

THERMAL CONDUCTIVITY OF PELLETS

The thermal conductivity was determined by measuring the temperature at the center as a function of time after the surface is exposed to an elevated, constant temperature. The used pellets were employed. A pellet initially at a uniform temperature of approximately 25°C. was immersed, at $\theta = 0$, in a wax bath maintained at a constant temperature of 170°C. The thermocouples on the surface and at the center of the pellet were connected to form a differential couple whose electromotive force was a direct measure of the difference in temperature. The wax did not appear to penetrate the pores during the time of the run (maximum $\theta = 90$ sec.). The ΔT was measured as a function of time.

If ΔT_o is the initial difference between surface and center temperatures and α the thermal diffusivity, the solution of the conduction equation, with α assumed constant, is (5)

$$\frac{\Delta T}{\Delta T_o} = 2\left(e^{-\pi^2\alpha\theta/R^2} - e^{-4\pi^2\alpha\theta/R^2} + e^{-9\pi^2\alpha\theta/R^2} - \cdots\right) \quad (2)$$

To avoid the inaccuracy in the value of ΔT_o, Equation (2) was applied to subsequent sets of two readings at later time values. When one notes that only the first term of the series is needed because of rapid convergence, and designates the temperature differences corresponding to θ_1 and θ_2 as ΔT_1 and ΔT_2, Equation (2) becomes

$$\alpha = \frac{\ln \dfrac{\Delta T_1}{\Delta T_2}}{\pi^2 \Delta\theta / R^2} \quad (3)$$

where $\Delta\theta = \theta_2 - \theta_1$.

The density of the pellet was known, and the specific heat at an average temperature could be calculated from the specific heats of the pure components. At 100°C. this was computed to be 0.18 cal./g. °C. From this information and α, given by Equation (3), the average value of k_e was estimated. Two runs were made with each pellet, and measurements were made with two pellets at each density level. The results are shown plotted vs. density in Figure 4.

The values of k_e must be regarded as approximate because rather simple instrumentation was used to measure ΔT vs. θ. The magnitude of the errors are indicated by the comparison between duplicate runs in Figure 4. Probably k_e is known to about ± 10%. Since other uncertainties in the prediction of the effectiveness factor introduce larger errors, these results are satisfactory.

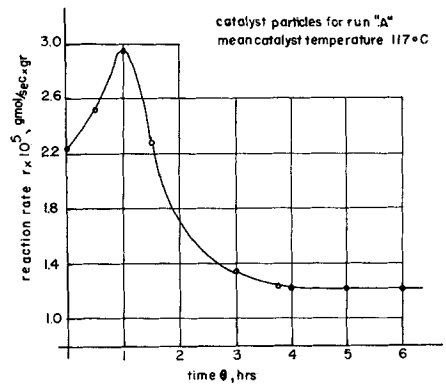

Fig. 3. Variation of catalyst activity with time.

It is of interest to compare these results with data for other catalysts, because little information is available for these kinds of materials. Sehr (25) studied dehydrogenation, reforming, and cracking catalysts and found k_e ranged from 5.3 to 8.6 $\times$ 10^{-4} cal./(cm.)(°C.)(sec.). Masamune and Smith (18) report data for aluminum oxide (Boehmite) and silver pellets as a function of void fraction. For $\epsilon_a = 0.3$, these values are about 4.1 $\times$ 10^{-4} cal./(cm.)(°C.)(sec.) for aluminum oxide (Boehmite) and 8.2 $\times$ 10^{-4} for silver. Figure 4 indicates that the values for the copper-magnesium oxide are a little lower. For example, for the pellet of comparable void fraction (ρ_B = 1.19 g./cc.) k_e from Figure 4 is 3-4 $\times$ 10^{-4} cal./(cm.)(°C.)(sec.).

CATALYST PRETREATMENT AND PRECISION OF RATE DATA

The oxide form of the catalyst was reduced in situ by passing a stream of hydrogen through the reactor at a rate of 100 cc./min. The reduction was considered complete when evaluation of water vapor ceased. This required about 8 hr. Preliminary experiments were carried out with different feed compositions and temperatures to study the variation of rate of reaction with time. A satisfactory aging procedure was finally found. This consisted of passing a 15 mole% ethylene (85% hydrogen) stream through the reactor for a period of several hours with the bath temperature at 110°C. The temperature within the catalyst initially rose to 150° to 180°C. and then gradually declined to a constant value of about 117°C. The rate, after the initial period of several hours, remained constant during the remainder of the test period, the longest of which was 3 days. A typical curve of rate vs. time for catalyst particles in the tubular reactor is shown in Figure 3. Discussions about the changes occurring during the aging process have been given by Wynkoop and Wilhelm (39) and Hall and Emmett (12), among others.

With this pretreatment procedure it was possible to obtain reproducible rate data. The rate for the catalyst particles was measured with three separate samples, run prior to, during, and after the measurements made with catalyst pellets. The data, all shown in Figure 5, agreed within 10%. For the pellet rate measurements, two pellets were prepared and studied kinetically at each of the two density levels of 0.72 and 1.16 g./cc., and three pellets were used at ρ_B = 0.95 g./cc. These data are shown on the pellet curves in Figure 5.

The constant rate observed after an initial interval, as shown in Figure 3, indicates that carbon deposition did not affect the steady state kinetic results. Perhaps the rapid decrease in activity during the initial time interval was due to a buildup of carbon, and when this reached a constant value, the rate of hydrogenation also became constant.

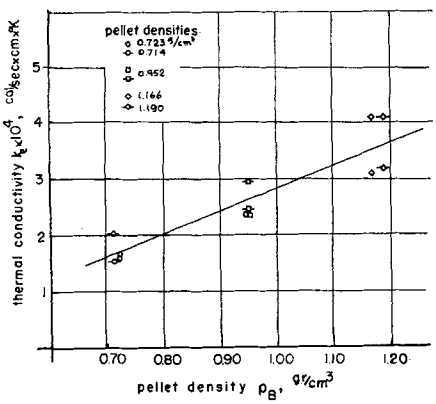

Fig. 4. Thermal conductivity of catalyst pellets.

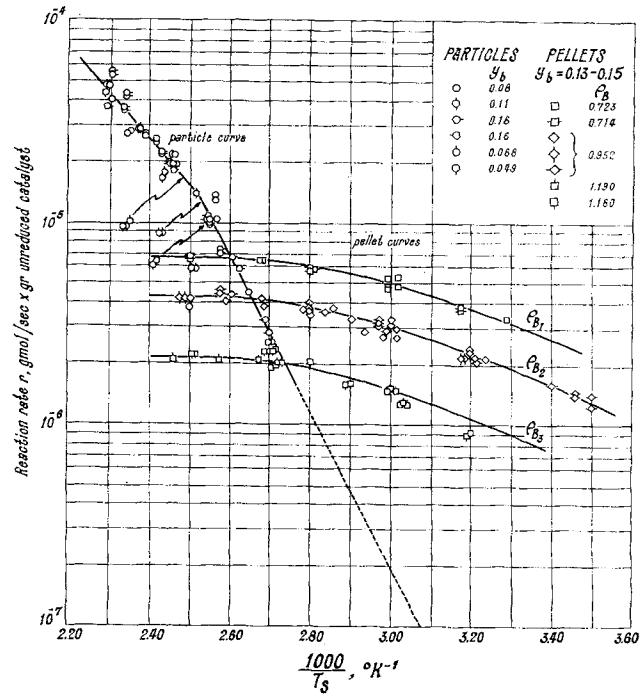

Fig. 5. Reaction rate results for particles and pellets.

SCOPE OF REACTION DATA

The rate measurements were carried out at the following conditions:

Pressure:
atmospheric
Temperature:
93° to 164°C. (catalyst particles)
12° to 134°C. (catalyst pellets)
Feed composition:
(C_2H_4 and H_2)
5 to 17 mole% C_2H_4 (catalyst particles)
13 to 15 mole% C_2H_4 (catalyst pellets)
Pellet density, ρ_B:
0.71 to 1.19 g./cc. (unreduced catalyst)
Conversion, x:
0.1 to 2.4% (moles reacted per total moles feed)

The objective of the study was not to evaluate a rate equation at the catalyst surface. Hence no attempt was made to operate over a wide range of pressure or feed composition. It was sufficient to measure rates of reaction for particles and pellets at the same conditions.

REACTION RATE RESULTS

Catalyst Particles

Owing to the low conversion the tubular reactor could be considered a differential type. The rate was calculated for each run from the conversion in the exit stream, the feed rate, and mass of catalyst. If F is the total feed rate

$$F\,dx = r\,dW \tag{4}$$

From the stoichiometry of the reaction, the mole fraction ethane is related to the conversion by the expression

$$x = \frac{y_e}{1 + y_e} \tag{5}$$

In terms of y_e Equation (4) becomes

$$r = \frac{F}{(1 + y_e)^2}\left(\frac{dy_e}{dW}\right) \tag{6}$$

Since the conversion is small, Equation (6) can be integrated with an arithmetic average value for $1/(1 + y_e)^2$.

Hence the rate is

$$r = \left[\frac{1}{(1+y_e)^2}\right]_{avg} \frac{F}{W} y_{e_0} \qquad (7)$$

where y_{e_0} is the measured mole fraction of ethane in the exit gas. This equation was used to calculate the rates of reaction for the catalyst particles.

The major uncertainty in the results so obtained is the temperature which corresponds with the rate. From the observed thermocouple readings the temperature distribution along the axis of the bed was estimated at the center and at the tube wall. From the wall and central axis temperatures a mean bed value at each bed depth was evaluated by assuming a parabolic radial gradient. This procedure was found to represent well the radial temperature distribution in a packed bed catalytic reactor by Hall and Smith (*13*). Then the length-mean temperature was taken as the correct temperature to correspond to the rate computed from Equation (7). This approximate but rapid procedure was checked for three extreme runs in the following way. From the preliminary results a plot of rate of reaction vs. temperature was prepared. This plot was used with the observed temperatures to obtain the rate as a function of radial and axial position in the bed. An average rate for the total mass of catalyst in the bed was then evaluated. These rates for the three runs were in excellent agreement with the experimental values from Equation (7). Table 2 gives some of the data obtained, and all the results are shown in Figure 5.

The particle data show a decrease in activation energy as the temperature goes above 120°C. This decrease has been observed in prior work (*10, 16, 23*) and has been explained on the basis of decreased adsorption of hydrogen, or alternatively, by postulating a competing reaction for ethylene at the higher temperatures. The activation energy in the low-temperature region from the authors' data is 17,800 cal./g. mole in comparison with 13,600 reported by Wynkoop and Wilhelm (39) for the same catalyst and 13,200 cal./g. mole by Pease (*20, 21*) for a copper foil catalyst. Drawing upon the vast literature pertaining to catalytic hydrogenation of ethylene (*9*), one can anticipate a general rate law of the form

$$r = \frac{k_1 K_1 C_{H_2} C_b}{1 + K_1 C_b} \qquad (8)$$

The temperature dependency noted by the authors and others is explicible in terms of Equation (8). In the low-temperature region $K_1 C_E >> 1$, and the rate equation reduces to

$$r = k_1 K_1 C_{H_2} C_b = A' C_{H_2} C_b \exp\left[-\frac{E}{RT}\right] \qquad (9)$$

With increasing temperature, ethylene coverage decreases, $K_1 C_b < 1$, and

$$r = k_1 K_1 C_{H_2} C_b = A' C_{H_2} C_b \exp\left[-\frac{(E-\lambda)}{RT}\right] \qquad (10)$$

where λ is an apparent heat of adsorption, not to be identified with calorimetrically determined chemisorption heats. These limits reveal that the experimental activation energy is a function of temperature itself and varied in this work from $E = 17{,}800$ to $E - \lambda = 11{,}800$.

The limiting second-order behavior at high temperature is verified since the rate, noted from the particle data in Figure 5, is an increasing function of ethylene concentration at temperatures above 120°C. In this temperature range comparison of particle and pellet rates (for example in obtaining effectiveness factors) were made at equal ethylene concentrations.

Catalyst Pellets

If the gas surrounding the pellet is of constant composition equal to that of the exit stream, the rate of reaction for the pellet is given by

$$r = \frac{F}{W} x_0 = \frac{F}{W}\left(\frac{y_{e_0}}{1+y_{e_0}}\right) \qquad (11)$$

This expression was used to calculate rates of reaction for the catalyst pellets from the observed values of y_{e_0}, F, and W. The results are illustrated for a few runs in Table 2, and all the data are shown in Figure 5 on the pellet curves. The temperature associated with each reaction rate is that of the surface of the pellet. The pellet curves in Figure 5 reveal singular behavior for each density, and all pellet rate data suggest a small activation energy which approaches zero at temperatures beyond 120°C.

When the temperature reaches a high enough value to make pore diffusion resistances significant, the apparent activation energy decreases to one half the true value. Weisz and Hicks (37) have shown that when temperature

TABLE 2. TYPICAL RATE DATA FOR CATALYST PARTICLES AND PELLETS

Total feed rate, g. moles/(sec.) × 10^4	Ethylene in feed, mole %	Ethane in exit gas, mole %	Conversion, x	Rate × 10^5, g. moles/sec. g.*	Mean bed temperature, °C.		
Mass of catalyst particles in bed = 0.115 g.*							
2.28	16.4	1.87	0.0086	1.99	133.6		
2.28	16.4	0.14	0.0014	0.32	98.6		
Mass of catalyst particles in bed = 0.0722 g.*							
2.52	11.2	1.16	0.0114	3.98	162.2		
2.57	11.6	0.52	0.0052	1.85	136.4		
Pellet density* = 0.723 g./cc.					Center	Surface	Gas
3.13	14.0	1.87	0.0184	5.18	75.0	59.6	59.4
2.10	14.9	2.42	0.0236	6.58	113.0	101.5	98.2
Pellet density* = 0.952 g./cc.							
2.06	13.0	1.07	0.0105	2.15	59.0	39.0	39.0
2.05	14.5	1.94	0.0190	3.88	118.8	102.0	100.4
Pellet density* = 1.190 g./cc.							
1.93	13.1	0.73	0.0073	1.12	57.0	43.9	43.6
1.99	13.5	1.35	0.0133	2.11	147.0	132.8	129.4

* Based upon mass of unreduced catalyst.

gradients exist in the catalyst pellet, the maximum decrease in apparent E for an exothermic reaction is still one-half the activation energy of the surface reaction. These conclusions are based upon the assumption that diffusion of reactants occurs in the gas phase of the pores simultaneously with heat transfer and reaction. Because of the more pronounced reduction of activation energy shown in Figure 5, simultaneous gas-phase diffusion and reaction in the pores cannot explain the results.

A pure diffusion resistance separated from reaction could explain a decrease in apparent E to essentially zero at high temperatures. Calculations were made to determine the magnitude of the diffusion resistance in the gas phase surrounding the catalyst pellet. These calculations were based upon the observed ΔT between gas and surface (Table 2). These ΔT values were from 0° to 3°C., and at these conditions the concentration change across the gas film is estimated to be not more than a few percent of the gas-phase concentration. Hence, it was concluded that external diffusion was not a significant factor.

However, there are several possible explanations for the observed behavior. First, the particle data (Figure 5) show that the rate decreased when the ethylene concentration fell below about 8 mole %. Since the mole fraction in the gas phase for the pellet work was 13 to 15%, the ethylene content near the center of the pellet is likely to have been less than 8 mole %. At higher temperatures the reduction in ethylene within the pellet would have been more severe than at lower ones. These factors could cause the decrease in E shown in Figure 5, and appear to be a likely explanation.

Surface diffusion rates usually decrease with temperature. If the mass transfer of reactants within the pellet is determined more by surface migration along the pore walls than in the gas phase, the total diffusion rate would decrease as the temperature increases. This behavior has been reported recently with ethyl alcohol on silica gel (*17*). Under these circumstances the observed rate of reaction could reverse the normal trend and actually decrease with temperature.

A third possibility is based upon the fact that the pellet curves in Figure 5 could be explained by a rate-controlling step of a diffusive nature. While resistances external to the pellet cannot be significant, a nonreactive, but permeable outer layer of catalyst can greatly reduce the rate. Also, the coking tendency on ethylene hydrogenation catalysts is well established. To achieve stable, steady state behavior in ethylene hydrogenation, the metal catalyst must be baked in ethylene to establish acetylenic residues upon that surface. Hydrogenation then occurs on the remaining uncoked sites. Figure 3 illustrates the rate behavior of the system during and after such treatment.

The location of the coked residues within the catalyst particle is governed by the reaction-diffusion parameters during pretreatment. If the coking occurred primarily near the outer surface of the pellet, this coked shell would constitute a purely diffusive resistance acting in series with the catalytic resistance in the active core. In contrast, if the coking were uniform in the pellet there is no possibility of a completely diffusive resistance. The two extremes of coke deposition, uniform and selective (pore mouth), are analogous to Wheeler's classifications for catalytic poisoning (*38, 1*).

EFFECTIVENESS FACTORS

Experimental Values

The pellet curves in Figure 5 give the rate of reaction at the surface temperature for gas compositions of 13 to 15 mole % ethylene. It has been mentioned that the external mass transfer resistances were negligible for the pellet reactor. Calculations for the catalyst particles also indicate that there was essentially no concentration difference between the gas phase and the surface of the particles. Furthermore, estimates in accordance with the procedure of Wakao and Smith (*34*) show that the effectiveness factor of the catalyst particles was unity. Therefore, the ratio of the pellet and particle rate data in Figure 5, at the same temperature, give experimental effectiveness factors for pellets of the three density levels. To the right of the particle line η is greater than unity, while to the left η is less than 1.0. It is noted that the rate per mass of catalyst increases as the density goes down. This indicates that the effect of a lower diffusion resistance in the larger pores of the least dense pellet more than offsets the effect of a lower thermal conductivity. Hence the temperature at which the intraparticle diffusion and heat transfer effects balance each other (intersection of pellet and particle curves) occurs at a higher temperature for the least dense pellet. Thus the effectiveness factor is unity at the following conditions:

Pellet density, g./cc.	Temperature °C.
0.72	111
0.95	102
1.17	92

For optimum reactor design a high reaction rate per unit volume of pellet is required. This rate is the product of the rate plotted in Figure 5 and the pellet density. Comparison on this basis brings the curves for the three densities closer together, but the highest value is still obtained with the least dense pellet. Hence an optimum density, if it exists for this nonisothermal system, would occur at a value less than 0.72 g./cc. Isothermal data for nickel on aluminum oxide catalysts for the ortho-para hydrogen conversion have demonstrated the existence of an optimum rate at a specific density (*6*).

Experimental effectiveness factors are given in the last column of Table 3. At temperatures below 93°C. the results are based upon extrapolation of the straight line (Figure 5) for the catalyst particles. Hence, the very high values at the lowest temperatures, for example $\eta = 25$ at $t = 60$°C. and $\rho_B = 0.72$ g./cc., are uncertain. However, there is little doubt that effectiveness factors much greater than unity existed for these operating conditions.

Table 3. Experimental and Predicted Effectiveness Factors

Pellet density, g./cc.	Temp., °C.	Φ	β	γ	Effectiveness factor η^*	η_c†	η (Exp.)
0.72	60	0.20	0.85	27	2000	23.0	25.0
	80	0.52	0.82	26	1000	5.0	6.7
	100	1.1	0.71	24	250	1.1	2.0
	120	2.2	0.70	23	150	0.3	0.6
0.95	60	0.27	0.50	27	200	16.0	14.5
	80	0.60	0.46	26	100	3.6	3.9
	100	1.3	0.41	24	30	0.86	1.2
	120	2.6	0.41	23	15	0.23	0.4
1.16	60	0.30	0.28	27	—	5.9	7.0
	80	0.66	0.27	26	20	2.7	2.0
	100	1.4	0.23	24	10	0.6	0.6
	120	2.8	0.22	23	5	0.2	0.2

* From Weisz-Hicks charts (*37*).
† From Equation (17).

Predicted Effectiveness Factors

Given the evidence of intraparticle temperature gradients in the pellet studies (Tables 2 and 4), nonisothermal effectiveness correlations should be used in an attempt to predict the experimental effectiveness factors. Unfortunately available correlations are not applicable for rate expressions suitable for the hydrogenation of ethylene, for example, Equation (8). The difficulty can be illustrated by applying the procedures of Weisz and Hicks (37) which are based upon a first-order binary reaction system. The required parameters are

$$\Phi = R\sqrt{\frac{\rho r}{C_s D_e}} \tag{12}$$

$$\beta = \frac{C_s(-\Delta H)D_e}{k_c T_s} \tag{13}$$

$$\gamma = \frac{E}{R_g T_s} \tag{14}$$

The particle rate data provide r and E; C_s is the hydrogen concentration at the pellet surface, and k_c is given in Figure 4 as a function of pellet density. The rate is evaluated at the pellet surface temperature T_s. Assuming negligible surface diffusion, D_e was computed by published methods (33) using the pore size and void fraction data available in Table 1. Diffusivities ranged from about 3 to 6×10^{-3} sq.cm./sec., depending upon density and temperature.

The predicted values of η from the Weisz ad Hicks charts are given in Table 3 (third from last column). The very high η for the lower-density pellets are in the region of β values such that stable effectiveness factors are beyond the charts; the tabulated values were obtained by extrapolation. The great excess of the predicted results over the experimental values is most likely due to the first-order, binary reaction restriction. This is particularly serious for our reaction. At the outer surface of the pellet where the ethylene mole fraction is 13 to 15% the rate is first order with respect to hydrogen and the charts are applicable. However, ethylene is the limiting component and towards the center of the pellet its concentration becomes low enough to reduce and control the rate. This reduction in rate results in a much lower effectiveness factor than predicted from the Weisz and Hicks charts.

A coked layer of inactive catalyst at the surface of the pellet would also cause a large reduction in effectiveness factor. However, experimental evidence indicates that this is not as likely an explanation as the incompatability of the first-order rate equation with the ethylene hydrogenation reaction. Thus one may calculate, using only the particle rate data in Figure 5, a hypothetical maximum rate of reaction in the pellet. Such a rate would occur at the center of the pellet if there were no diffusion resistance. This means that the ethylene mole fraction would be the same as at the outer surface of the pellet, or the same as that upon which the particle rata data are based. Therefore the maximum rate at the center would be the value read from the particle rate curve in Figure 5 at the center temperature. The ratio of this rate to that evaluated at the surface temperature gives an upper limit for the effectiveness factor. These maximum effectiveness factors were calculated from the measured temperatures, for example as illustrated for a few runs in Table 2. The results ranged from 2 to 20, which is much lower than the predicted values in Table 3 and of the same order as the experimental results. While the maxima are approximate because of the difficulty in accurately measuring center temperatures, this comparison does suggest that the low effectiveness factors are not due to a coked outer layer on the pellet.

Table 4. Temperature Difference Between Surface and Center of Catalyst Pellet

Pellet density, g./cc.	Surface temp., °K.	$(T_c - T_s)$, °C. Max. (calc.)	Exp.
0.72	300	37.4	16.6
	400	41.0	13.0
0.95	300	23.0	20.0
	400	24.2	16.0
1.16	300	17.5	14.0
	400	17.8	15.0

While it is not a plausible explanation of the data in this case, a purely diffusive resistance in series with the catalytic processes can have a large influence on the effectiveness factor. Simply to demonstrate a quantitative procedure for measuring the effect, this concept is applied to our data in the following section.

Influence of Pore Mouth Poisoning

Suppose that an inactive outer layer of thickness z surrounds the active core of the spherical catalyst pellet. Let η be the effectiveness factor of the active core and η_o be the observed overall value. Since the rate of reaction is equal to the diffusion rate through the coked layer,

$$A D_e \frac{C_s - C_f}{z} = \eta k_1 C_f \tag{15}$$

where C_f is the concentration at the boundary between active core and coked layer. In this equation the rate constant k_1 is equivalent to $\rho r/C_f$. Here r is the particle rate of reaction and C_f is the reactant concentration at the coked pore-active catalyst boundary. Expressing the rate for the pellet in terms of C_s

$$r = \frac{\eta k_1 \rho C_s}{1 + \left(\frac{\eta k_1 \rho}{(A D_e/z)}\right)} = \eta_o k_1 \rho C_s \tag{16}$$

Overall effectiveness is then

$$\eta_o = \frac{\eta}{1 + \frac{\eta k_1 \rho}{(A D_e/z)}} \tag{17}$$

In Equation (17), η is obtained from the Weisz-Hicks charts which assumes the reaction is first order in hydrogen throughout the pellets. The quantity $A D_e/z$ must be estimated. To evaluate η with this model, the parameters Φ, β and γ should be calculated at conditions corresponding to the coked pore-active catalyst boundary. In particular the temperature T_f will be different from T_s and, in general, it would be necessary to write an energy balance to evaluate it. Further the diffusivities and thermal conductivities of coked layer and active catalyst are not identical. Hence it is not possible to predict accurate values of Φ, β, and γ or of $A D_e/z$.

However, the effect of the model on reducing the effectiveness factor can be approximated by simplifying the situation. We first assume Φ, β, and γ are the same as obtained by neglecting the coked layer. These values and the resulting η are given in Table 3. Then $A D_e/z$ is arbitrarily chosen to be 0.1 sec.$^{-1}$ in order to give good agreement between predicted η_o values and the experimental effectiveness factors. The η_o results, calculated from Equation (17) taking $A D_e/z = 0.1$ sec.$^{-1}$ and $k_1 = r\rho/C_s$ are given in the next to the last column of Table 3. To obtain this value of $A D_e/z$, $D_e = 10^{-3}$ sq.cm./sec. and $z = 0.5$ mm. Comparison of the η and η_o results shows the severe effect of a purely diffusive resistance in the outer layer of the pellet.

Maximum Temperature Difference

A final point of interest is the magnitude of the observed temperature differences between the surface and center of the pellets. Damkoeler (7, 8) and later Weisz and Prater (36) have shown that this temperature difference, $(T_s - T_c)$ is given by the following expression, regardless of the reaction rate equation:

$$T_s - T_c = \frac{(-\Delta H)(D_e)}{k_e}(C_c - C_s)$$

The center concentration C_s is not known. However, a maximum ΔT can be estimated by taking $C_s = 0$. The values of $(T_s - T_c)_{max}$ and the corresponding experimental values are shown in Table 4 for the three catalyst densities. The observed ΔT is less than the maximum value, as expected, for all cases. The difference increases as the pellet density decreases. One explanation for this is the decrease in diffusion resistance as the density decreases. This means that the actual concentration at the center of the pellet is further removed from zero as the density decreases and hence, ΔT from Equation (12) deviates more from the actual value.

ACKNOWLEDGMENT

The assistance of the National Science Foundation for part of the financial requirements of this research is gratefully acknowledged.

NOTATION

A = surface to volume ratio for sphere = $3/R$
a = pore radius, cm.
C = gas-phase concentration, g. moles/cc.
C_f = gas-phase concentration at boundary between coked layer and active catalyst, g. moles/cc.
C_p = specific heat of catalyst, cal./(g.)(°C.)
D_e = effective diffusivity of catalyst pellet, sq.cm./sec.
E = activation energy, cal./g. mole
F = total feed rate, g. moles/sec.
ΔH = heat of reaction, cal./g. mole
K_1 = adsorption coefficient
k_1 = first-order (hydrogen) rate constant, $sec.^{-1}$
k_e = effective thermal conductivity of catalyst pellet, cal./(sec.)(cm.)(°C.)
R = radius of spherical catalyst pellet, cm.
R_g = gas constant, cal./(g. mole)(°K.)
r = reaction rate, g. mole/(sec.)(g. unreduced cat.)
S = surface area, sq. m.
T = temperature, °K.
V = pore volume, cc.
W = mass of catalyst, g.
x = conversion, moles of ethylene reacted per mole of total feed
y = mole fraction
z = length of coked pore, cm.

Greek Letters

α = thermal diffusivity, $k_e/c_p\rho_B$, sq.cm./sec.
β = dimensionless group defined by Equation (13)
γ = dimensionless group defined by Equation (14)
ϵ = void fraction
η = effectiveness factor of catalyst pellet: (rate of reaction per pellet)/(rate at surface conditions)
Φ = Thiele type of modulus, defined by Equation (12)
ρ = catalyst density, g./(cc. of unreduced catalyst)
θ = time, sec.

Subscripts

a = macropores (radius > 150Å)
B = pellet
b = ethylene
c = ethane, or center of pellet
f = boundary between coked layer and active catalyst
g = per gram
i = micropores (radius < 150Å)
o = outlet of reactor
p = particle
s = surface of pellet

LITERATURE CITED

1. Barnett, L. G., R. E. C. Weaver, and M. M. Gilkeson, *A.I.Ch.E. Journal*, 7, 211 (1961).
2. Buben, N. Ya., *J. Phys. Chem. USSR*, **19**, 250 (1945).
3. Carberry, J. J., *A.I.Ch.E. Journal*, 8, 557 (1962).
4. *Ibid.*, 7, 350 (1961).
5. Carslaw, H. S., and J. C. Jaeger, "Conduction of Heat in Solids," Oxford at the Clarendon Press, England (1958).
6. Cunningham, R. E., and J. M. Smith, *A.I.Ch.E. Journal*, 9, 419 (1963).
7. Damkoehler, G., *D. Chem. Ing.*, 3, 430 (1937).
8. ———, *Z. physikal. Chem.*, **A193**, 16 (1943).
9. Eley, D. D., "Catalysis," P. H. Emmett, ed., Vol. 3, Reinhold, New York (1956).
10. Farkas, A., and L. Farkas, *J. Am. Chem. Soc.*, **60**, 22 (1938).
11. Frank-Kamenetskii, D. A., *Zh. Tekh. Fiz.*, 9, 1457 (1937).
12. Hall, W. K., and P. H. Emmett, *J. Phys. Chem.*, **63**, 1102 (1959).
13. Hall, R. E., and J. M. Smith, *Chem. Eng. Progr.*, **45**, 459 (1949).
14. Kubota, H., and M. Shindo, *Chem. Eng. (Japan)*, **20**, 11 (1956); 23, 284 (1959).
15. ————————, *Can. J. Chem. Eng.*, **39**, 127 (1961).
16. Lewis, J. R., and J. S. Taylor, *J. Am. Chem. Soc.*, **60**, 877 (1938).
17. Masamune, Shinobu, and J. M. Smith, *A.I.Ch.E. Journal*, to be published.
18. ————————, *J. Chem. Eng. Data*, 8, 54 (1962).
19. Mingle, J. O., and J. M. Smith, *A.I.Ch.E. Journal*, 7, 243 (1961).
20. Pease, R. N., *J. Am. Chem. Soc.*, **45**, 1196, 2297 (1923).
21. ———, and C. A. Harris, *ibid.*, **49**, 2503 (1937).
22. Prater, C. D., *Chem. Eng. Sci.*, 8, 284 (1958).
23. Reinacker, G., and E. A. Bommer, *Z. anorg. allgem. Chem.*, 236 263 (1938).
24. Schilson, R. E., and N. R. Amundson, *Chem. Eng. Sci.*, **13**, 226 (1961).
25. Sehr, R. A., *ibid.*, 9, 145 (1958).
26. Taylor, E. H., *J. Am. Chem. Soc.*, **63**, 2906 (1941).
27. *Ibid.*, p. 2911.
28. Taylor, H. S., and G. G. Joris, *Bull. soc. Chim. Belge.*, **46**, 457 (1954).
29. Thiele, E. W., *Ind. Eng. Chem.*, **31**, 316 (1939).
30. Tinkler, J., and R. L. Pigford, *Chem. Eng. Sci.*, **15**, 326 (1961).
31. ———, and A. B. Metzner, *Ind. Eng. Chem.*, **53**, 663 (1961).
32. Wagner, K., *Z. physikal. Chem.*, **A193**, 1 (1943).
33. Wakao, Noriaki, and J. M. Smith, *Chem. Eng. Sci.*, **17**, 825 (1962).
34. ————————, *Ind. Eng. Chem. Fund. Qrtly.*, 3, 123 (1964).
35. Weisz, P. B., *Z. physikal. Chem. Neue Folge*, **11**, 1 (1957).
36. ———, and C. D. Prater, "Advances in Catalysis," Vol. 6, p. 143, Academic Press, New York (1954).
37. ———, and J. S. Hicks, *Chem. Eng. Sci.*, **17**, 265 (1962).
38. Wheeler, A., "Catalysis," P. H. Emmett, ed., Vol. 2, Reinhold, New York (1955).
39. Wynkoop, R., and R. H. Wilhelm, *Chem. Eng. Progr.*, **46**, 300 (1950).
40. Zeldovich, J. B., *Acata. Physicochim. USSR*, **10**, 583 (1939).

Manuscript received February 10, 1964; revision received May 7, 1964; paper accepted May 11, 1964. Paper presented at A.I.Ch.E. San Francisco meeting.